Melanoma Skin Cancer Detection using ANN

Glòria Macià Muñoz

227-1040-00L Theory, Programming and Simulation of Neuronal Networks by Prof. Dr. Ruedi Stoop

Abstract

Malignant melanoma is the most dangerous form of skin cancer, but early diagnosis plays an essential role in the control and cure of the disease. In this paper, a computer-based system to classify histopathological images of skin tissue using artificial neural networks is implemented. Performance measures of the proposed system are encouraging and there is no evidence of overfitting. Therefore, an extended version of this system could be used to assist hospital pathologists and increase the efficiency of our healthcare system.

ETH Zürich, Spring Semester 2017

Introduction

In recent years, national health care spending has grown at rates well below the historical average. In the US, for instance, health care costs rise faster than inflation as can be seen below [1].

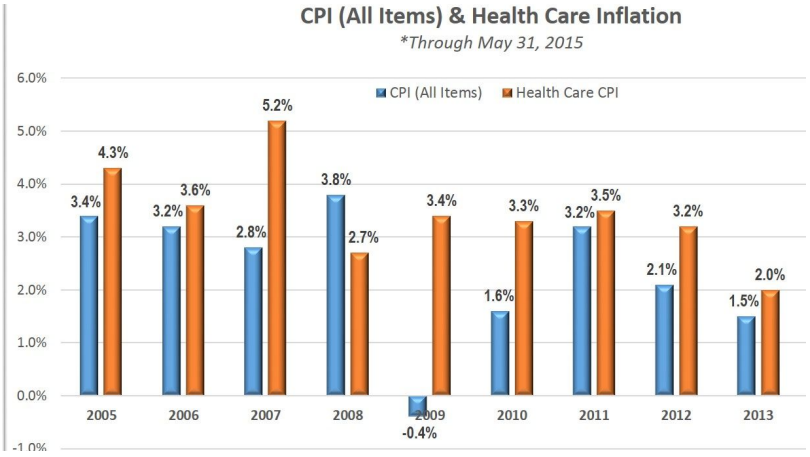

Figure 1: Percentage increase in overall inflation as measured by the consumer price index (all items) and health care inflation from 2005 through May 31, 2015. Notice how health care inflation has outpaced the CPI in each year except 2008 [1].

Among many other suggestions to slow down health care inflation, hospitals should eliminate waste and increase efficiency to reduce operating costs [2]. An example of such inefficiencies is the process of diagnosing simple but high-frequency cases such as malignant melanoma. Malignant melanoma is the most dangerous form of skin cancer, but early diagnosis plays an essential role in the control and cure of the disease.

According to the American Cancer Society's estimates [3] for melanoma in the United States for 2017 are the following:

- About 87,110 new melanomas will be diagnosed (about 52,170 in men and 34,940 in women).
- About 9,730 people are expected to die of melanoma (about 6,380 men and 3,350

On any given day, hospital pathologists inspect a large number of samples like one provided below, and their visual assessment relies on delicate patterns.

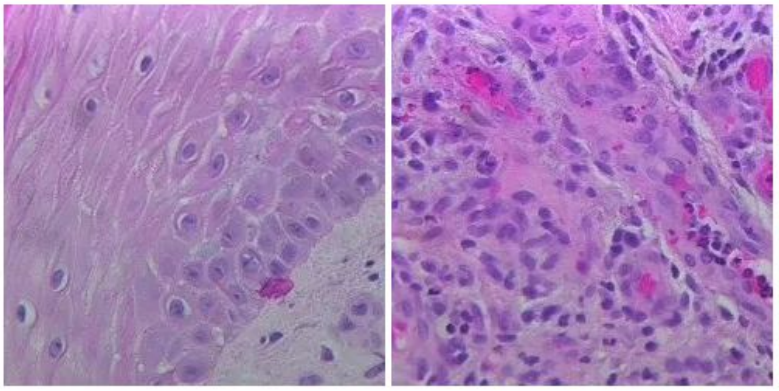

Figure 2: Histological images of skin tissue obtained using an optical microscope with an 400x lense. Samples were hematoxylin-eosin stained during Mohs surgery. On the left, a portion of normal skin tissue. On the right, a malignant melanoma cancerous sample.

The goal of this scientific paper is to design a computer-based system to classify histopathological images of skin tissue. Notice that the proposed system is by no means intended to substitute pathologists but to help them so that they can spend their limited time better and, thinking globally, ease the burden of the national health service from countries all around the world.

Disclaimer

The dataset used in this project was provided by the Pathology Unit – Hospital del Mar – Parc de Salut Mar (Barcelona, Spain) [4] and must be used solely for the purpose of research and education. The same applies to the Neural Network Classifier which has not undergone the CE marking regulatory process for medical and in vitro diagnostic devices in the European Unit [5].

In addition, advanced image processing and feature extraction was required prior to designing the classifier in *Mathematica.* This work has been done in *Matlab* by the same author who enroll in *227-1040-00L Theory, Programming and Simulation of Neuronal Networks* course [6] by Prof. Dr. Ruedi Stoop to learn how to implement a Neural Network Classifier and be able to understand its efficiency characteristics.

Methods

1. Dataset Generation

- **Histological image data**

Histological images of skin tissue were obtained using an optical microscope with an 400x lense. Samples were hematoxylin-eosin stained during Mohs surgery, a surgical technique that consists on removing thin layers of skin with cancer while simultaneously analyzing it in the microscope so that the tumor is removed progressively until only healthy tissue remains.

A total of 100 instances (49 healthy samples and 51 samples with malignant melanoma) were provided as dataset by the Pathology Unit – Hospital del Mar – Parc de Salut Mar (Barcelona, Spain).

- **Image Processing**

Prior to designing the neural network, image processing and feature extraction was required.

Histological images were automatically cropped to get rid of margins and converted into gray-scale. Next, the cell nuclei were extracted using a simple thresholding algorithm (i.e. based on its intensity (I), a pixel was classified as nuclei ($I<120=1$) or cytoplasm ($I\geq120=0$)). In order to isolate the nuclei from other small low intensity components, all connected components of the image that had less than 30 pixels were removed. Finally, to improve the automatic

segmentation and fill the holes in the segmented and yet keep the nuclei size unchanged a binary dilation followed by binary erosion was performed. This whole process is depicted in **Figure 3**.

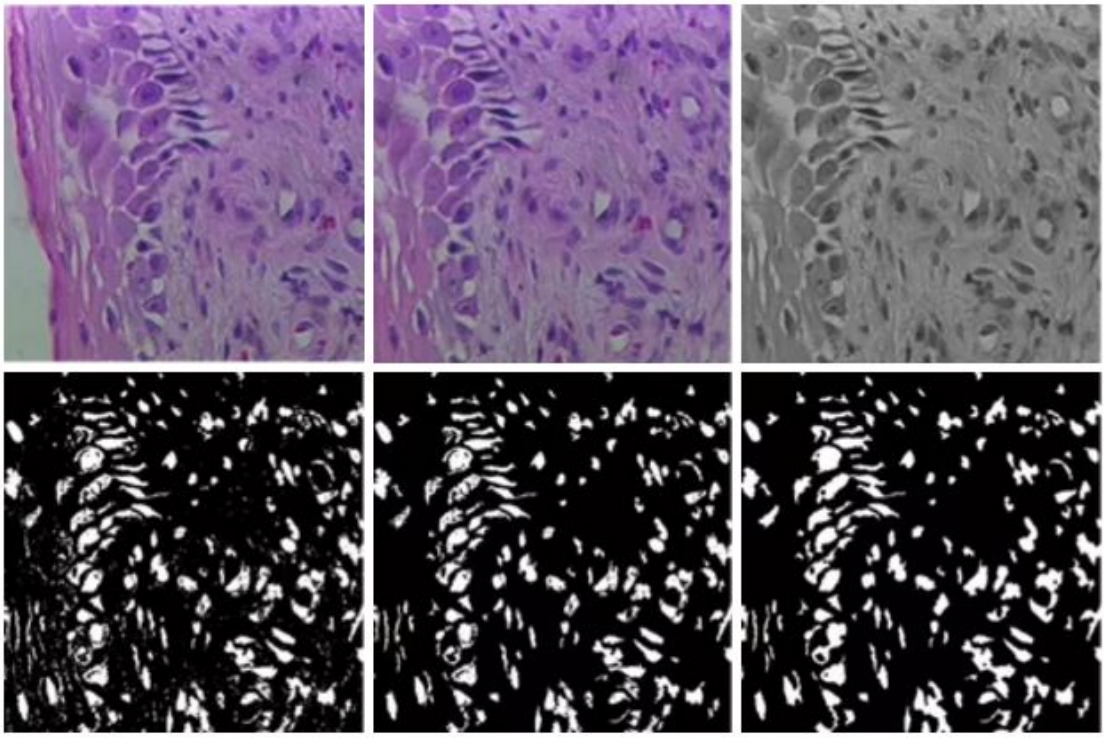

Figure 3: Histological image data processing. From upper left to bottom right: original histological sample, cropped sample, grayscale image, thresholded image, connectivity analysis performed and resulting image.

- **Feature Extraction**

  Cancer is characterized by the abnormal and uncontrolled growth of cells and how these invade adjacent tissues. The properties of cancerous tissues are observed by pathologists through histological analysis and used for diagnosis purposes. In this research, three main tissue features were extracted for the subsequent classification task: nuclear-cytoplasmic ratio, nuclei number and pleomorphism (size variance).

  For illustrative purposes, an excerpt from the .xlsx file is provided below (**Table 1**) together bivariate scatter plots (**Figure 4)**. An in-depth explanation of how these tissue features are obtained is also provided in the *supplementary materials.*

NCR	Nuclei Count	Size variance	Label
0,1231	69	1.03E+09	0
0,1117	60	1.77E+08	0
0,0986	57	1.54E+09	0
...	...	...	...
0,3125	128	5.61E+09	1
0,2950	156	1.65E+09	1
0,2041	109	1.97E+09	1

Table 1: Excerpt from the .xlsx file containing the three input features for the classifier plus the ground truth label. In the ground truth label column, 0 corresponds to a normal image sample whereas 1 corresponds to a cancerous one.

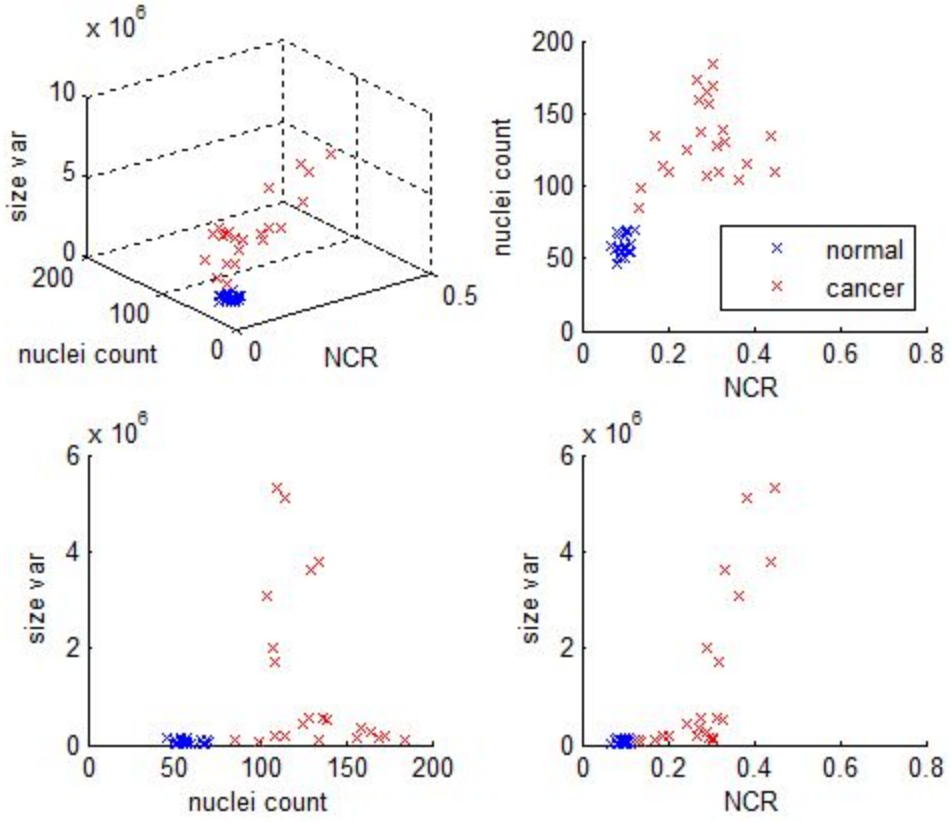

Figure 4: Feature space in the three features' dimensions and plane projections. Instances correspondent to normal images are represented in blue, while instances of cancer images are represented in red.

2. Artificial Neural Network Classifier

- **Importing Data - Training & Testing Set**

  The data stored in the .xlsx file is imported into Mathematica and divided between inputs and target. Out of the one hundred samples, seventy will be randomly selected and used for training the Artificial Neural Network (ANN). The remainder will be used to evaluate its performance afterwards.

- **Defining the ANN with one hidden layer**

  An Artificial Neural Network (ANN) is an information processing paradigm inspired by the way biological nervous systems, such as the brain, process information [7]. Neural networks are typically organized in layers made up of a number of interconnected 'nodes' which contain an 'activation function'. Patterns are presented to the network via the 'input layer', which communicates to one or more 'hidden layers' where the actual processing is done via a system of weighted 'connections'. The hidden layers then link to an 'output layer' where the answer is output [8]. In this paper, an ANN with three input units, one hidden layer with three hidden units and one output unit is built. Such an ANN is shown in **Figure 5.**

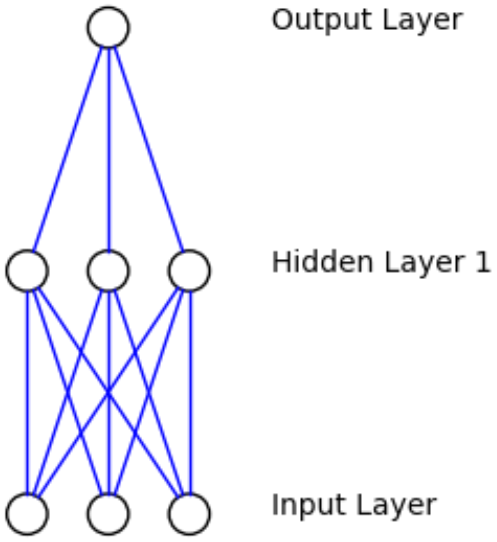

Figure 5: Artificial Neural Network (ANN) architecture.

- **Training the ANN**

  Most ANNs contain some form of 'learning rule' which modifies the weights of the connections according to the input patterns that it is presented with. Among the many different kinds of learning rules, here the delta rule was used. This rule is frequently utilized by the most common class of ANNs called 'backpropagational neural networks' (BPNNs). In this class of ANNs, learning is a supervised process that occurs with each cycle or 'epoch' (i.e. each time the network is presented with a new input pattern) through a forward activation flow of outputs, and the backwards error propagation of weight adjustments [8].

To keep track of the training process, the squared error was computed for every image in the training set. Although some images have higher error values than others, it can be clearly seen in **Figure 6** how the training error decreases after every cycle.

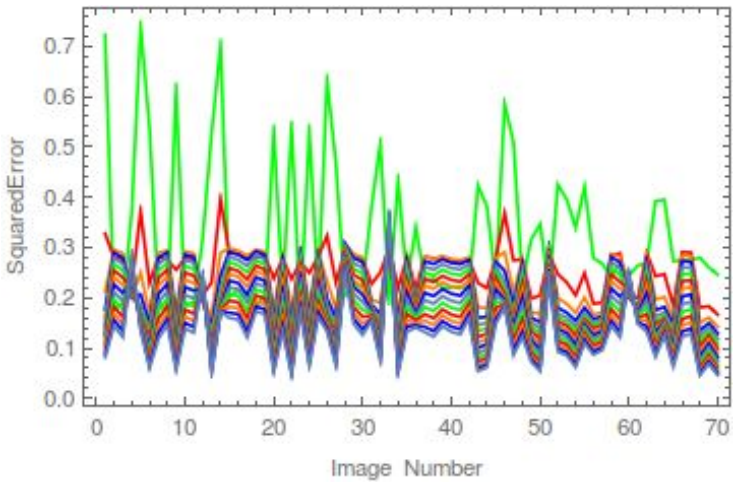

Figure 6: Squared Error for each image in the training set (training set size = 70) decreases epoch after epoch. A total of 15 iterations are done for every image.

Results and Discussion

The testing set (testing set size = 30) has been used to evaluate the previously trained ANN. To do so, the following performance measures have been calculated: sensitivity, precision, specificity and accuracy. The obtained values are shown in **Table 2.**

Performance Measure	Value
Sensitivity	1
Precision	0.933
Specificity	0.933
Accuracy	0.966

Table 2: Performance values of the trained ANN in a randomly selected run of the Mathematica code.

Since our classifier seemed to be performing so well, the possibility of overfitting needed to be ruled out. In overfitting, a statistical model describes random error or noise instead of the underlying relationship. Overfitting occurs when a model is excessively complex, such as having too many parameters relative to the number of observations. Such a model has poor predictive performance, as it overreacts to minor fluctuations in the training data. In simple words, overfitting occurs when a model begins to "memorize" training data rather than "learning" to generalize from trend [9].

To asses overfitting, the Root Mean Squared (RMS) Error was plotted against the iteration number for both the training and the testing set. As can be seen in **Figure 7**, both the

training and testing error decrease simultaneously so there is no evidence of overfitting in our model.

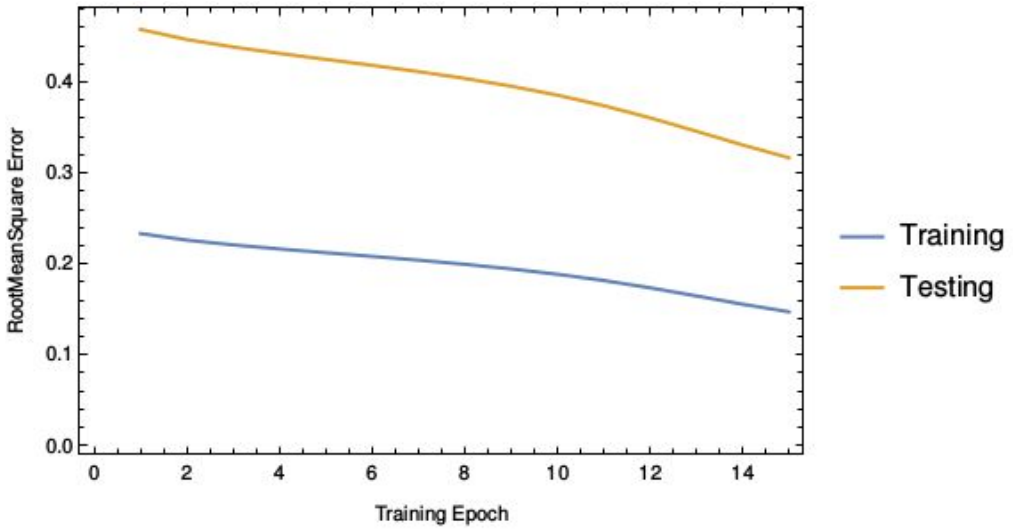

Figure 7: Root Mean Squared (RMS) Error of the ANN classifier plotted at every epoch for both the training and testing set.

Conclusions

In this paper it has been shown that it is indeed possible to design a computer-based system to classify histopathological images of skin tissue using ANN. Even though the proposed system has not undergone the European CE marking regulatory process for medical devices, performance measures are very encouraging and there seems to be no evidence of overfitting. Hence, an improved version of such a system could be used to assist pathologists in their day-to-day hospital tasks so that they can spend their limited time better and contribute to increase the efficiency of our healthcare system.

Bibliography

1. Patton M. U.S. Health Care Costs Rise Faster Than Inflation. Forbes. https://www.forbes.com/sites/mikepatton/2015/06/29/u-s-health-care-costs-rise-faster-than-inflation/#1d9013c96fa1. Published June 29, 2015. Accessed June 1, 2017.

2. 4 Ways Hospitals Can Solve the Problem of Rising Healthcare Costs. Health Catalyst. https://www.healthcatalyst.com/hospitals-solve-rising-healthcare-costs. Published June 3, 2017. Accessed June 1, 2017.

3. Key Statistics for Melanoma Skin Cancer. American Cancer Society. https://www.cancer.org/cancer/melanoma-skin-cancer/about/key-statistics.html. Accessed June 1, 2017.

4. Hospital del Mar. Hospital del Mar - Parc de Salut Mar. https://www.parcdesalutmar.cat/hospitals/hospital-del-mar/en_presentacio.html. Accessed June 7, 2017.

5. WM-. Guidelines for Classification of Medical Devices - CE Marking (CE Mark) for Medical Devices - EU Council Directive 93/42/EEC. Guidelines for Classification of

Medical Devices - CE Marking (CE Mark) for Medical Devices - EU Council Directive 93/42/EEC. http://www.ce-marking.org/Guidelines-for-Classification-of-Medical-Devices.html. Accessed June 7, 2017.

6. 227-1040-00L Theory, Programming and Simulation of Neuronal Networks. ETH Zurich - Course Catalogue. http://www.vvz.ethz.ch/Vorlesungsverzeichnis/lerneinheitPre.do?lerneinheitId=112257&semkez=2017S&lang=en. Accessed June 7, 2017.
7. 文章. http://www.doc.ic.ac.uk/~nd/surprise_96/journal/vol4/cs11/report.html# - Open Access Library. http://www.oalib.com/references/7680507. Accessed June 12, 2017.
8. A Basic Introduction To Neural Networks. A Basic Introduction To Neural Networks. http://pages.cs.wisc.edu/~bolo/shipyard/neural/local.html. Accessed June 12, 2017.
9. Overfitting. Wikipedia. https://en.wikipedia.org/wiki/Overfitting. Published June 9, 2017. Accessed June 12, 2017.
10. S.J. Keenan, J. Diamond, W.G. McCluggage, H. Bharucha, D. Thompson, P.H. Bartels, P.W. Hamilton, An automated machine vision system for the histological grading of cervical intraepithelial neoplasia (CIN), Journal of Pathology 192 (3) (2000) 351–362.

11. M. Guillaud, K. Adler-Storthz, A. Malpica, G. Staerkel, J. Matisic, D.V. Niekirkd, D. Cox, N. Poulina, M. Follen, C. MacAulaya, Subvisual chromatin changes in cervical epithelium measured by texture image analysis and correlated with HPV, Gynecologic Oncology 99 (2005) S16–S23.

12. He, L. et. al. (2012). Histology image analysis for carcinoma detection and grading. Computer methods and programs in biomedicine , 538–55

13. J. Monaco, J. Tomaszewski, M. Feldman, M. Moradi, P.cMousavi, A. Boag, C. Davidson, P. Abolmaesumi, A. Madabhushi, Detection of prostate cancer from whole-mount histology images using Markov random fields, in: Workshop on Microscopic Image Analysis with Applications in Biology, 2008.

14. J. Monaco, J. Tomaszewski, M. Feldman, M. Mehdi, P. Mousavi, A. Boag, C. Davidson, P. Abolmaesumi, A. Madabhushi, Probabilistic pair-wise Markov models: application to prostate cancer detection, SPIE Medical Imaging 7259 (2009) 725903-1–725903-12.

Supplementary Materials

Feature Extraction

In this research, three main tissue features were extracted for the subsequent classification task: nuclear-cytoplasmic ratio, nuclei number and pleomorphism (size variance). An in-depth explanation of how these tissue features are obtained is also provided below.

Nuclear-Cytoplasmic ratio

The nuclear-cytoplasmic ratio (NCR) is a measurement used in cell biology. It is a ratio of the size (i.e. volume) of the nucleus of a cell to the size of the cytoplasm of that cell. The NCR has already been noticed as a distinguishing feature in other studies of epithelial computer-based analysis for cancer identification [10, 11] since due to uncontrolled growth of cells the amount of nuclei and its DNA content increases abnormally [12].

The NCR can be calculated by dividing the number of 1s present in the binary image, which represent the nuclei pixels, by the total image size (i.e. the sum of 0s and 1s present in the binary image matrix).

Nuclei number

As previously mentioned, it the amount of nuclei increase as the uncontrolled growth of cancer happens [12]. The number of nuclei is the count of foreground connected components in an 8-pixel neighborhood.

Pleomorphism

Pleomorphism, as used in histology, describes the variability of size, shape and staining of cells. The additional content of DNA in cancerous cells changes its form and size [12]. Size and variance of nuclei have been used as a characteristic feature to classify cancerous tissue in several studies [13, 14].

Since the number of nuclei was already known from the section above, the only task remaining was to count the amount of pixels in each nuclei and compute for every image sample the variance of its nuclei sizes vector.